



Optimization of 3D phase contrast venography for the assessment of the cranio-cervical venous system at 1.5 T

Mona Salehi Ravesh^{1,2} · Ulf Jensen-Kondering² · Julia Juhasz² · Sönke Peters² · Monika Huhndorf² · Joachim Graessner³ · Thomas W. D. Möbius⁴ · Marcus Both² · Olav Jansen² · Jan-Bernd Hövener¹

Received: 22 October 2018 / Accepted: 3 December 2018 / Published online: 4 January 2019
© Springer-Verlag GmbH Germany, part of Springer Nature 2019

Abstract

Purpose The aim of this work was to optimize a three-dimensional (3D) phase-contrast venography (PCV) product MR pulse sequence in order to obtain clinically reliable images with less artifacts for an improved depiction of the cranio-cervical venous vessels.

Methods Starting from the product sequence, the 3D PCV protocol was optimized in eight steps with respect to the velocity encoding (V_{enc}) direction and value, slice thickness, reduction of susceptibility artifacts and arterial contamination, gradient mode and radio-frequency (RF)-spoiling, B_0 -Shimming, asymmetric echo technique and RF-pulse type, and flip angle. The product and optimized protocol was used to perform 3D PCV in 12 healthy male volunteers with a median age of 50 years using a state-of-the-art 1.5-T MR system. For evaluation, the cranio-cervical venous system was divided into 15 segments. These segments were evaluated by three radiologists with experience in neuroradiology. An ordinal scoring system was used to assess the overall diagnostic quality, arterial contamination, and the quality of visualization.

Results Image quality in the optimized 3D PCV was graded as “excellent” by all readers in 65.3% of the cases ($p < 0.0001$). The visualization of venous segments was strongly improved: it was considered diagnostic in 81.8% of all cases using the optimized sequence and in 47.6% for the product 3D PCV ($p < 0.0001$), respectively. The optimized protocol improved the imaging of all venous segments ($p < 0.0001$).

Conclusion The optimized 3D PCV pulse sequence showed superior results compared to the product 3D PCV for the visualization and evaluation of the venous system in all healthy volunteers.

Keywords Magnetic resonance imaging (MRI) · Non-contrast-enhanced venography · 3D phase contrast magnetic resonance imaging (PCV-MRI) · Pseudotumor cerebri · Cerebral venous thrombosis

Electronic supplementary material The online version of this article (<https://doi.org/10.1007/s00234-018-2146-6>) contains supplementary material, which is available to authorized users.

✉ Mona Salehi Ravesh
Mona.Salehiravesh@uksh.de

¹ Section Biomedical Imaging, Molecular Imaging North Competence Center (MOIN CC), Department for Radiology and Neuroradiology, University Medical Center, Arnold Heller Street 3, Building 41, 24105 Kiel, Germany

² Department for Radiology and Neuroradiology, University Hospital Schleswig-Holstein, Campus Kiel, Kiel, Germany

³ Siemens Healthcare GmbH, Hamburg, Germany

⁴ Institute of Medical Informatics and Statistics, Kiel University, Kiel, Germany

Introduction

Diseases of the cranio-cervical venous system are rare but often underdiagnosed. Idiopathic intracranial hypertension (IIH), also known as pseudotumor cerebri, is a syndrome of increased cerebrospinal fluid (CSF) pressure. Diagnosis is based on clinical parameters [1, 2], increased CSF pressure (> 200 mm H₂O on lumbar puncture), and exclusion of cerebral mass lesions and venous thrombosis [1]. On cerebral imaging, the majority of patients displays venous outflow restriction (VOR), most apparent in the transverse sinuses but detectable in the entire venous tree [3, 4]. Follow-up after treatment can demonstrate VOR reversal and treatment success.

Cerebral venous thrombosis (CVT) is an uncommon cause of stroke, accounting for approximately 1% of all strokes, and more frequently seen in younger patients [5]. Headache is the

leading clinical symptom [6] and may be associated with signs of ischemia or hemorrhage. Diagnosis requires imaging confirmation of an occluded vein [7]. Vessel recanalization should be documented after therapy.

Clear visualization and precise delineation of the cranio-cervical venous vessels are thus paramount for the diagnosis and follow-up after treatment in patients with IIH and CVT. Venous digital subtraction angiography (DSA), computed tomography (CT) venography, and contrast-enhanced magnetic resonance angiography (CE-MRA) are standard procedures to visualize cerebral venous vessels. However, DSA is invasive and carries a potential procedural risk. Furthermore, DSA and CT utilize harmful ionizing radiation, which should be avoided. All techniques mentioned above require an iodine or gadolinium-based contrast agents with rare but possibly life-threatening side effects such as renal impairment, thyrotoxicosis and allergic reactions, nephrogenic systemic fibrosis, and cerebral gadolinium deposition [8–10] and allergic reactions for the latter. Thus, a non-invasive, contrast-agent-free imaging method without ionizing radiation would be beneficial for the safety of patient and practitioner alike.

Non-contrast-enhanced magnetic resonance imaging (MRI) techniques, such as conventional time-of-flight (TOF) angiography [11] and three dimensional phase contrast venography (3D PCV) and susceptibility weighted imaging (SWI) [12] fulfill these requirements. These methods are thus of high interest for the evaluation of the cranio-cervical venous system in the clinical routine. This is especially true for the typical cohort of patients with suspected IIH or CVT and follow-up imaging after treatment.

The PCV MR technique is based on the effect that spins moving through a magnetic field gradient accumulate a different phase of magnetization (phase shift) compared to static spins. For PCV imaging, two interleaved images are acquired over successive repetition times with and without a bipolar magnetic field gradient along one spatial direction (x , y , or z). This bipolar magnetic field gradient only affects moving spins, which acquire a different phase based on their specific flow characteristics. The difference between the phase data of two successively acquired images (with and without flow-weighting gradients) is thus proportional to phase shifts from moving spins. The unique aspect of the PCV technique is that it provides a true velocity map, in which the voxel signal intensity values are proportional to the actual flow velocity in a particular flow direction along the x -, y -, or z -axis (velocity-encoded direction). The flow sensitivity of this technique can be adjusted using the determination of a maximum expected velocity encoding (V_{enc}) [13].

2D and 3D TOF venography are the first non-invasive MRI techniques that were used for intracranial venous evaluation. Liauw et al. [14] did not recommend the usage of 3D TOF venography due to severe in-plane signal intensity saturation and preferred 2D TOF or 3D PCV for an overall reliable and

visual better image quality and visualization of cortical veins [15]. Compared to TOF, 3D PCV allows variable velocity encoding and provides directional flow information [16].

However, we noted that the state-of-the-art product protocols of 3D PCV were suitable only for rough visualization of the sagittal sinus or transverse sinus (Syngo version E11C, Siemens Healthcare, Erlangen, Germany).

These protocols were limited with respect to the anatomical coverage of the entire cranio-cervical veins, the visualized blood flow directions, as well as the visualization of cranio-cervical veins for a reliable diagnosis of cranio-cervical venous disease.

The aim of this work was to improve the imaging of cranio-cervical venous vessels by optimizing the product 3D PCV protocol at 1.5-T MRI system.

Material and methods

Imaging hardware/software Imaging was performed on a state-of-the-art 1.5-T MRI system equipped with second-order shims (Magnetom Aera, XQ gradients, Siemens Healthcare, Erlangen, Germany) using a 20-channel head-neck coil (Siemens Healthcare, Erlangen, Germany). The MRI system was operated by the latest software (Syngo version E11C).

Imaging sequence Dumoulin et al. introduced the 3D PCV technique as a contrast agent-free method for the visualization of the vessel structures [17]. The 3D PCV sequence used in this work is based on the sequence design described by Hausmann et al. [18] from the manufacturer Siemens Healthcare.

Protocol optimization To obtain high quality 3D visualization of the cranio-cervical venous system, the product protocol was optimized with respect to the following points:

1. The number of V_{enc} directions was changed from two (anterior posterior and foot to head) to three (plus right to left) spatial directions.
2. The V_{enc} value in the product 3D PCV protocol was set to 20 cm/s. Using this value, the cranio-cervical veins were poorly resolved, e.g., compared to the sagittal sinus. To find an optimal V_{enc} value, which provides a clear visualization of most cranio-cervical veins, the blood flow velocity was measured in the sagittal and transverse sinus veins of two healthy male volunteers with different ages of 35 and 75.6 years. 2D PC flow MR images were acquired with a V_{enc} of 5–45 cm/s with an increment of 5 cm/s. The blood flow velocity was evaluated in the sagittal and transverse sinus veins in the direction of the flow (anterior to posterior and left to right, Figs. 1b and 2).

In these measurements, an electrocardiogram (ECG)-trigger was used instead of the peripheral pulse (PPU)-trigger. PPU is used for routine 2D PC flow MR measurements in the cerebral regions, but it is less accurate due to its inherent limitations for the detection of the R-wave compared to the ECG-trigger.

To make sure that the V_{enc} obtained with ECG-trigger is comparable with that using PPU-trigger, the 2D PC blood flow measurements were repeated in transverse sinus vein with one setting of $V_{enc} = 40$ cm/s, which is the clinical standard (Fig. 3). The PPU-trigger device was positioned on the index finger, and slices were planned perpendicular to the vessels (Fig. 1).

The 2D PC blood flow images using both ECG- and PPU-trigger were analyzed on the MR work station using a dedicated software provided by the manufacturer (Syngo-Argus, version A20B, Siemens Healthcare, Germany).

3. Slice thickness was reduced from 5.14 to 2.40 mm to obtain images with an interpolated spatial resolution of 1.2 mm. Additionally, “edge enhancement” with a smoothing factor of 3 was activated under “image filter.” The changes to the “image filter” parameter can be used to adjust the optimal intensity, edge enhancement, and smoothing of the MR-image
4. Reduction of susceptibility artifacts and arterial contamination: To suppress the cerebral arterial signal and to reduce susceptibility artifacts from the nose-mouth-region, a spatial saturation slab with a thickness of 75 mm was placed angulated about 120° to the carotid, nasal, and oral area of the subject on a sagittal view (Fig. 1a).
5. Gradient mode and radio-frequency (RF) -spoiling: The system allows operating the gradients in three different

modes (fast/normal/whisper) with the following parameters:

- Gradient maximum amplitude 24/22/22 [mT/m]
- Gradient minimum rise time 5.55/10/20 [μ s/(mT/m)]
- Gradient maximum slew rate 180.18/100/50 [mT/m/ms]

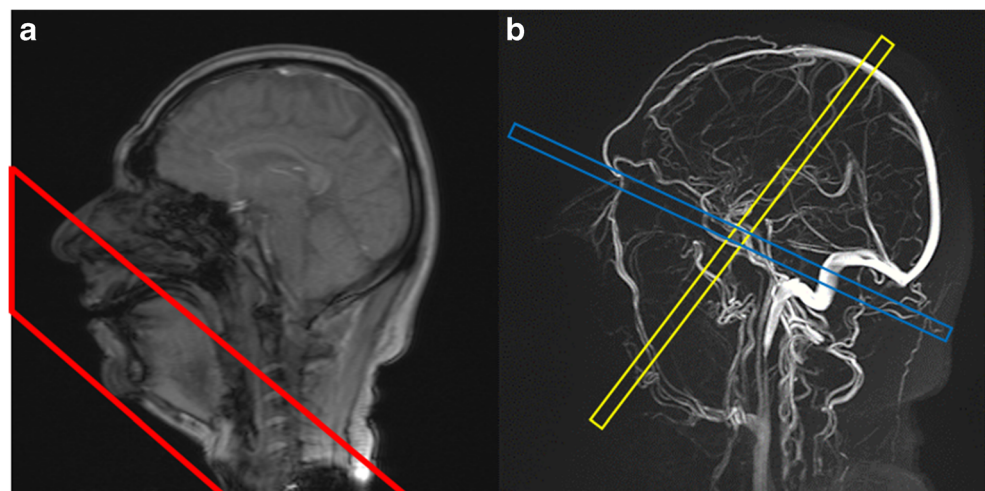
It was evaluated, if the “whisper” setting was suitable for 3D PCV to reduce acoustic noise [19].

RF-spoiling was activated to reduce the residual transverse magnetization after readout further (prior to the application of the next excitation).

6. B_0 -shimming: The system offers three modes to improve the homogeneity of the magnetic field (shimming): a fixed preset (“tune-up”), one iteration of a Double Echo Steady State (DESS) [20] (“standard”), and two iterations of DESS [20] (“advance”). In the product 3D PCV, the homogeneity was set to “tune up.” The “standard” shim setting [21] was used in the optimized 3D PCV protocol.
7. Asymmetric echo technique and RF-pulse type: The echo can be asymmetrically acquired with two strengths, “weak and strong” with a relative echo position of 36% and 23%, if this function is activated. Otherwise, the echo will be sampled symmetric. A symmetric readout refers to a relative echo position of 50%, whereas a fully asymmetric readout refers to 0%.

Asymmetric echo acquisition was deactivated in the optimized protocol compared to “weak” asymmetric echo in the product protocol. To avoid a prolongation of the echo-, repetition-, and thus total measurement time, the RF-pulse type was changed from normal to fast mode. Partial echo acquisition (asymmetric echo) allows to reduce the echo time

Fig. 1 **a** Illustrating the positioning of the saturation slab (red) on a sagittal view of a healthy volunteer. The saturation slab with a thickness of 75 mm suppresses the cerebral arterial signal intensity and the generated noise due to the different susceptibility region in the nose-mouth-region. **b** The blue and yellow slabs/bars show the planned slice for both ECG- and PPU-triggered 2D PC blood flow MRI measurements in the transverse and sagittal sinus veins



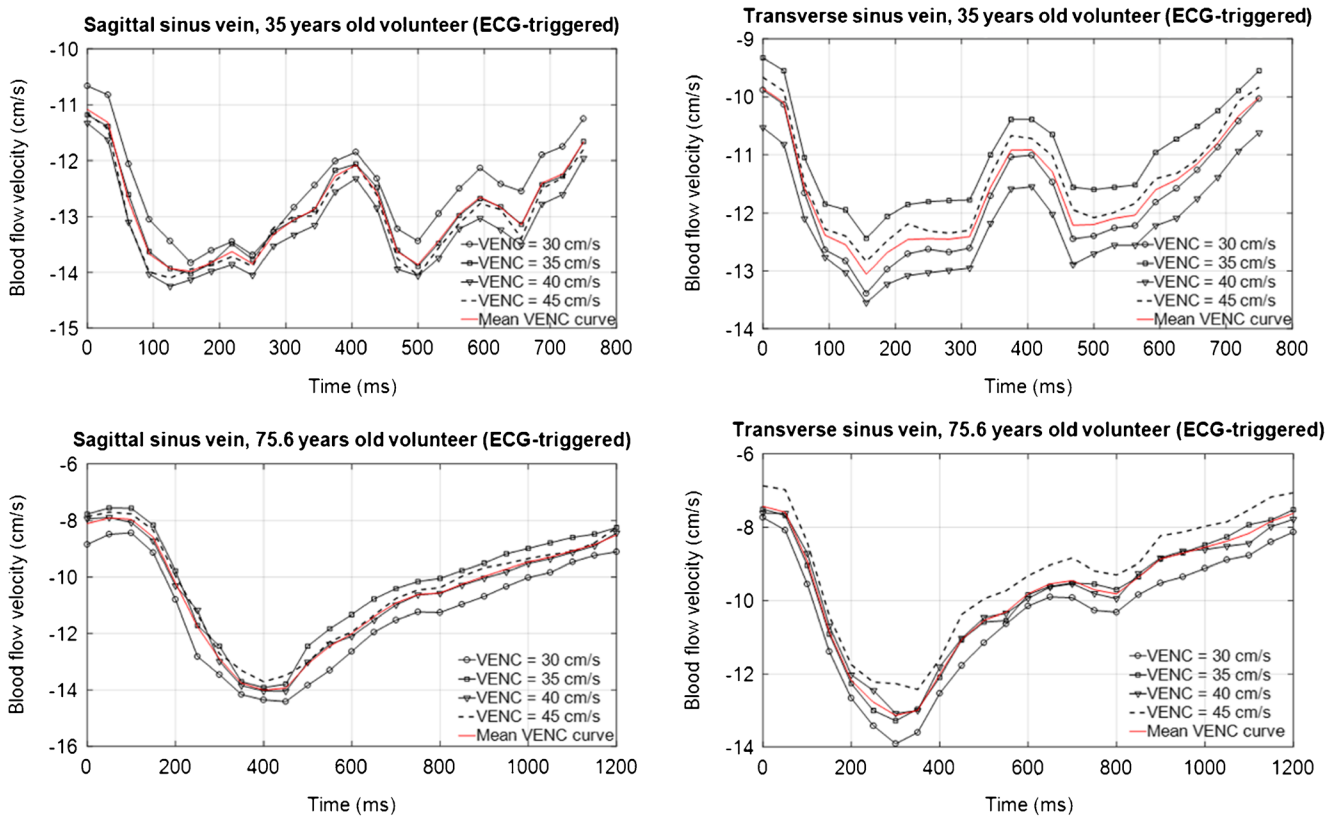


Fig. 2 Optimization of the V_{enc} value using ECG-triggered 2D PC blood flow MRI measurements in two healthy volunteers (35 and 75.6 years old). The measured blood flow velocities in the sagittal and transverse sinus veins (upper and lower row) with four V_{enc} -values are displayed as a

function of the time. The averaged curve (red line) in each of these four panels shows a maximal amplitude of below 15 cm/s. The reverse blood flow direction in the vein compared to that of an artery is indicated with a minus sign

compared to imaging with full echo acquisition. But the acquisition of only a fraction of the echo (data) leads to the reduction of the image signal-to-noise (SNR) in an image, which is a disadvantage for the visualization of the anatomical structure and distinguishing the signal intensity of the vein from the background [22].

The system offers to choose RF-pulses as “fast,” “normal,” and “low specific absorption ratio (SAR)” with a pulse length

of 1.28, 2.56, and 3.84 ms, respectively. The fast mode provides a shorter TE and TR, and also fewer susceptibility artifacts compared to the other two modes.

8. Flip angle: To optimize the flip angle, a series of measurements was performed with the optimized protocol using eight different flip angles between 5 and 25°. The resulting SNR was evaluated by dividing the mean signal

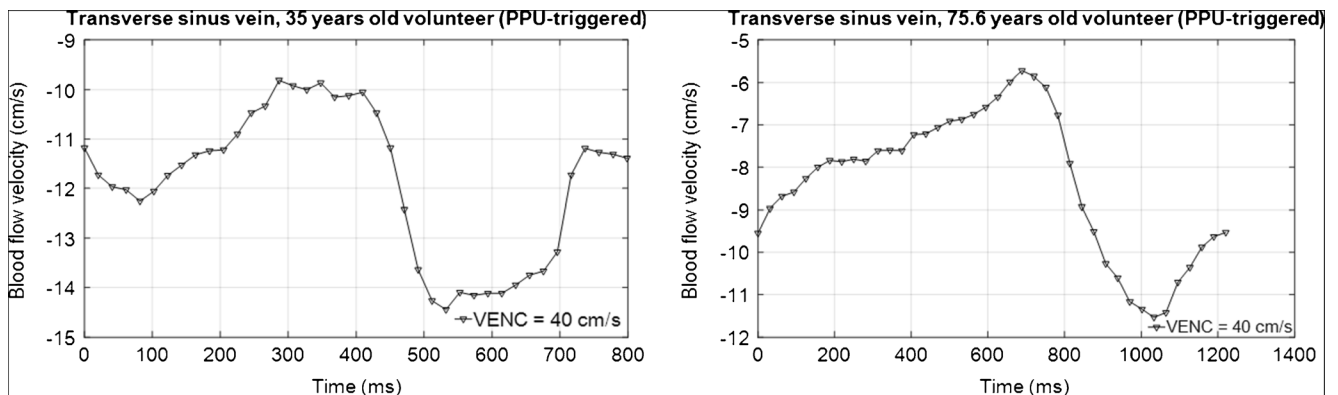
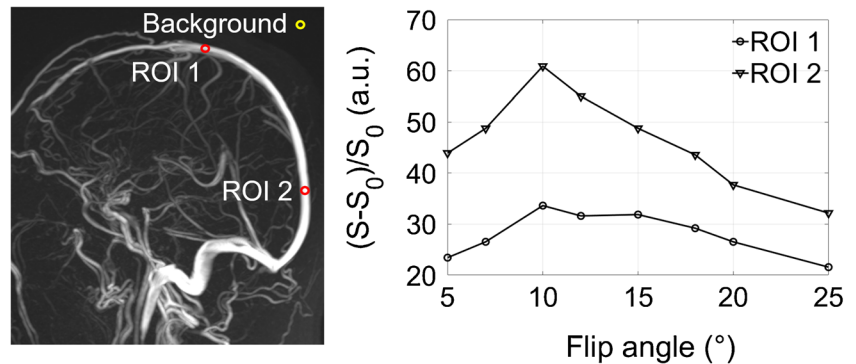


Fig. 3 Blood flow velocity in transverse sinus veins of two healthy volunteers (35 and 75.6 years old), acquired with PPU-triggered 2D PC blood flow MRI. The minus on the velocity scale indicates the reverse blood flow direction in the vein compared to that of an artery

Fig. 4 Optimization of the flip angle for 3D PCV. Left: Maximum-intensity-projection (MIP) of a 3D PCV and three same size region-of-interests (ROIs) in the sagittal sinus vein and in an apparently signal-free region. Right: The relative signal intensity changes of the ROI 1 and 2 to that of the background as a function of the flip angle. A flip angle of 10° was chosen for the optimized protocol



intensity of a region of interest (ROI) in the sagittal sinus and in a signal-free background (outside of the subject). All three ROIs had the same size (24 pixels, area = 0.06 cm^2 , Fig. 4).

To evaluate the image quality of the standard and optimized 3D PCV protocol, the following image protocol was applied to all volunteers: fast overview imaging (three orthogonal slices) T_1 - and T_2 -weighted MR images of the head in transversal slice orientation, 2D phase-contrast (PC) flow imaging, and 3D PCV.

Volunteers

The study population consisted of 12 healthy male volunteers (median, [min, max] of age, 49.7 [21.4, 75.6] years; weight, 77.0 [57.0, 105.0] kg; body mass index (BMI), 25.2 [20.2, 30.9] kg/m^2).

Evaluation

To evaluate the image quality of the cranio-cervical venous system, in particular, for IIH and CVT, the images acquired with the product and optimized 3D PCV protocol were evaluated for technical and clinical aspects based on three scoring systems [20, 23].

Three blinded board-certified radiologists (U.J.K., S.P., and J.J.) with at least 7 years of experience in neuroradiology analyzed all 12 data sets twice. The images were evaluated independently and during separate reading sessions. The first and second analysis was at least 4 weeks apart. The names of the volunteers and sequences were anonymized.

The image quality of 3D PCV images (Fig. 5) was rated by using a scoring scale of 1–3 with respect to the venous enhancement and presence of artifacts (including parallel acquisition reconstruction artifact, motion artifact, and/or noise):

- Grade 1: Poor image quality, inadequate venous enhancement, and/or the presence of a significant amount of artifacts/noise impairing the diagnosis.
- Grade 2: Good image quality sufficient for diagnosis, adequate venous enhancement, and/or mild-to-moderate amounts of artifacts/noise not interfering with diagnosis.
- Grade 3: Excellent image quality for highly confident diagnosis, good venous enhancement, and no-to-minimal amount of artifacts/noise.

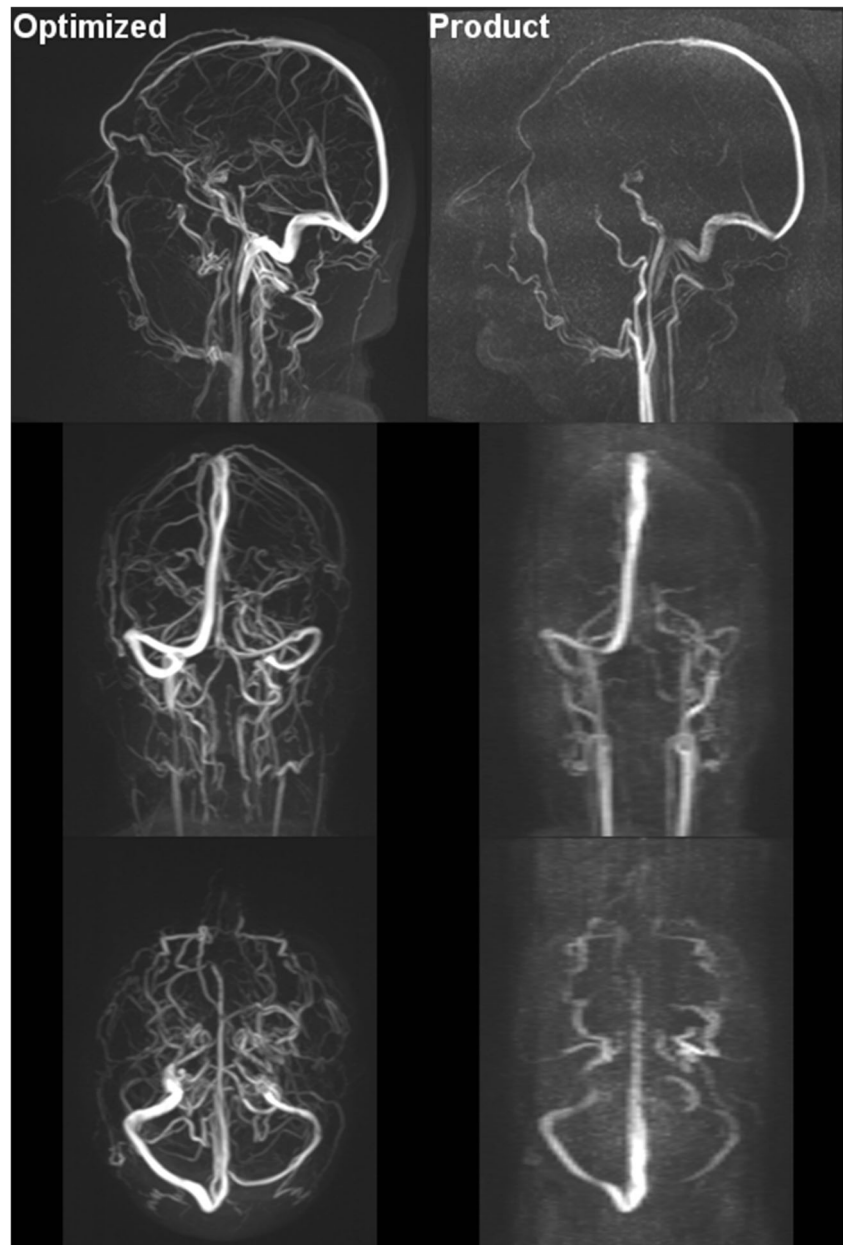
Potentially contaminating arterial enhancement was evaluated on a scale of 0–3:

- Grade 0: None.
- Grade 1: Minimal, allowing interpretation with a high degree of diagnostic confidence.
- Grade 2: Moderate, exceeding acceptable degree and limiting diagnostic confidence.
- Grade 3: Severe, markedly limiting diagnostic confidence.

The cranio-cervical venous system structures, including cerebral venous sinuses and major superficial and deep cerebral veins were divided into 15 segments (Fig. 6). The continuity, visibility, and edge sharpness of the cranio-cervical venous segments were assessed in each healthy volunteer. Visualization of venous structures was assessed by using a scoring scale of 1–4:

- Grade 1: Not visible.
- Grade 2: Partially visible, not sufficient for diagnosis.

Fig. 5 Exemplary maximum intensity projection (MIP) views of optimized (left side) and product (right side) 3D PCV depicting the visualized cranio-cervical veins of a healthy volunteer (51 years old). See [supplementary video](#)



- Grade 3: Generally homogenous enhancement and continuity of venous structure, sufficient for diagnosis.
- Grade 4: Excellent image quality with highly homogeneous and continuous enhancement and conspicuous sharpness of vessel border, allowing highly confident diagnosis.

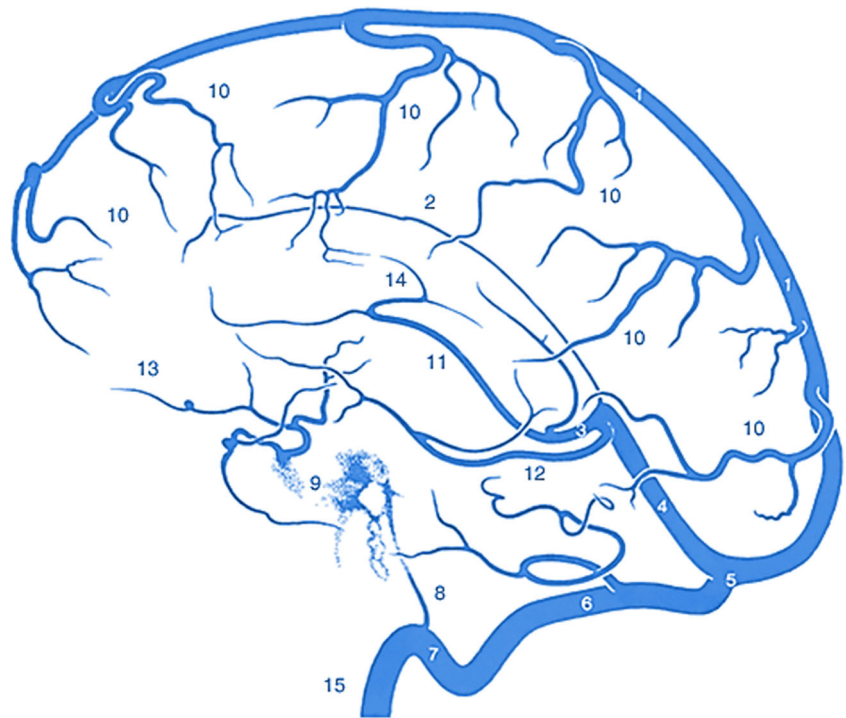
The image quality of a venous segment was rated as diagnostic (grade ≥ 3) if the reader was confidently able to visualize the lumen of the venous structure in its entirety.

Most of the examined venous segments in this study are bilateral. For the purpose of this study, only the dominant side was evaluated to avoid errors due to aplasia and asymmetries.

Data analysis

Median and range are reported as summary statistics for all variables due to the severe skewness of the respective distributions. Intra- and interrater agreement on the scoring of an image were assessed by quadratic weighted concordance [25]. A Wilcoxon Signed-Rank Test was used to evaluate whether the optimized 3D PCV sequence outperformed the product sequence. All p values were reported with a precision of 10^{-5} . A p value < 0.01 was considered statistically significant. Statistical analysis of the data was performed with R (R Statistic package, version 3.5.1, R Foundation for Statistical Computing, Vienna, Austria). Concordance was calculated with the raters package (CRAN: raters). Diagrams were

Fig. 6 Segmentation of the cranio-cervical venous system. The veins are marked as follows in the image: Superior sagittal sinus (1), Inferior sagittal sinus (2), Vein of Galen (3), Straight sinus (4), Torcular Herophili (5), Transverse sinus (6), Sigmoid sinus (7), Superior petrosal sinus (8), Cavemous sinus (9), Cortical veins (10), Internal cerebral vein (11), Basal vein of Rosenthal (12), Superior ophthalmic vein (13), Thalamostriate vein (14), Internal jugular vein (15). The figure is a modified illustration from reference [24] with permission



plotted with MATLAB (Version 2017a, The MathWorks, Natick, MA, USA).

The conventional interpretation of an agreement is as follows: <0.00 indicate poor agreement, 0.00–0.20 indicate slight agreement, 0.21–0.40 indicate fair agreement, 0.41–0.60 indicate moderate agreement, 0.61–0.80 indicate substantial agreement, and 0.81–1.00 indicate almost perfect agreement [26].

Results

All MRI-examinations were performed successfully. All datasets were included in the study.

Technical optimization of 3D PCV

1. The number of V_{enc} directions, the changing the number of V_{enc} directions from two to three allowed the encoding of the venous blood flow in all three spatial directions instead of only two. This led to the improvement of the vessel visualization.
2. The V_{enc} value: For $V_{enc} = 30\text{--}45$ cm/s, similar blood flow velocity profiles were measured using the ECG-triggered 2D PC flow MRI in the sagittal and transverse sinus veins of two healthy volunteers (Fig. 2). The maximum blood flow velocities in both volunteers did not exceed a value of 15 cm/s. Aliasing appeared for $V_{enc} = 5\text{--}25$ cm/s (data not shown).

The measured PPU-triggered 2D PC blood flow velocity-time curves of two volunteers (35 and 75.6 years old) are exemplary shown in Fig. 3. The median PPU-frequency of all 12 volunteers was 61.5 [49.0, 80.0] bpm. The median of blood flow velocity of all volunteers was -10.4 [-14.7 , -5.9] cm/s. Note, that the minus sign indicates opposite direction of the blood flow direction in the vein compared to that of in an artery.

Thus, for the optimized 3D PCV protocol, a $V_{enc} = 15$ cm/s was chosen.

3. The slice thickness was reduced from 5.4 mm to 2.4 mm (interpolated 1.2 mm) to obtain a sharp in-plane visualization of the vessel edges. The use of the image filter intensified the optical sharpness of the vessel edges (Fig. 5).
4. Reduction of susceptibility artifacts and arterial contamination: A used spatial saturation slab with a thickness of 75 mm in the optimized protocol provided an improved suppression of the susceptibility artifacts and contamination with signal from the arteries, resulting in an overall improved visualization of the veins (Fig. 5, nose-mouth-and neck-region).
5. Gradient mode and RF-spoiling, The “whisper” setting of the gradients mode did not restrict the 3D PCV sequence, but reduced the acoustic noise. The RF-spoiling contributed significantly to improving the visualization of the vessels (Fig. 5). Both features were added to the optimized protocol.
6. B_0 -shimming: compared to “tune-up” mode, using the “standard shim” as a shimming mode, the magnetic field

was homogenized subject-adapted for each individual volunteer before the running of a sequence is carried out.

7. Asymmetric echo technique and RF-pulse type: Asymmetric echo acquisition was turned off to acquire whole data (k-space), which was advantageous for the improving the visualization of the vessels. By using “fast” RF-pulses, TE was increased from 7.9 to 8.6 ms without visible impact on the image quality.
8. Flip angle, the maximum value of the relative signal intensity of the sagittal sinus vein to the background was achieved by a flip angle of 10° (Fig. 4).

The standard and optimized 3D PCV protocol parameters are summarized in Table 1.

Image quality

A total of 24 data sets (12 data sets and two analysis sessions) were evaluated per standard/optimized 3D PCV by all three readers.

For the product 3D PCV, reader 1 graded the overall image quality as poor and good in 20.8% (5/24) and 79.2% (19/24) of cases, reader 2 in 95.8% (23/24) and 4.2% (1/24) of cases, and reader 3 in 41.7% (10/24) and 58.3% (14/24) of cases.

For the optimized 3D PCV, reader 1 graded the overall image quality as “good” in 4.2% (1/24) and as “excellent” in 95.8% (23/24) of cases, reader 2 graded “good” in 100% (24/24) of cases, and reader 3 graded “excellent” in 100% (24/24) of cases. Median image quality in optimized 3D PCV was

Table 1 MR protocol parameters used in this study

	3D PCV MRI		2D PC flow MRI	
	Product	Optimized	ECG-triggered	PPU-triggered
TR/TE (ms)	37.3/7.9	74.4/8.6	117.7/7.6	22.9/7.1
Acquisition matrix (Px)	256 × 256 × 192	256 × 256 × 192	192 × 192	256 × 256
Acquisition voxel (mm ³)	1.30 × 0.98 × 5.14	1.30 × 0.98 × 2.40	1.8 × 1.8 × 6.0	0.63 × 0.63 × 5.0
Reconstruction voxel (mm ³)	0.49 × 0.49 × 3.00	0.49 × 0.49 × 1.2	1.8 × 1.8 × 6.0	0.63 × 0.63 × 5.0
Number of slices	64	160	1	1
Number of averages	1	1	1	1
V _{enc} (cm/s)			Through plane 5	
AP	20	15	to 45, with an	–
RL	–	15	increment of 5	–
FH	20	15		40
BW (Hz/Px)	300	300	440	201
FA (°)	15	10	20	10
Imaging orientation	Sagittal	Sagittal	Perpendicular to the vessel	Perpendicular to the vessel
Phase oversampling (%)	0	0	30	60
Filter	Distortion correction (2D); elliptical filter	Distortion correction (2D); prescan normalizer; elliptical filter; image filter (edge enhancement/smooth factor: 3/3)	Off	Elliptical filter
B ₀ shim mode	Tune-up	Standard	Tune-up	Standard
Asymmetrical echo	Weak	Off	Strong	Weak
RF pulse type	Normal	Fast	Fast	Normal
Gradient mode	Fast	Whisper	Normal	Fast
RF spoiler	Off	On	On	
Flow compensation	Off	Off	On	On
Integrated parallel imaging techniques (iPAT) PAT modulus (acceleration factor/reference lines)	GRAPPA (2/24)	GRAPPA (2/24)	GRAPPA (2/24)	GRAPPA (2/32)
Saturation slab (mm)	–	75	–	–
Trigger delay (sec)	–	–	0	0
Acquisition time (min)	2:51	10:44	0:15	3:44

Table 2 Intra observer agreement for the evaluation of image quality, arterial contaminating, and visualization of all venous segments of product and optimized 3D PCV based on the introduced 3- and 4-point

Variable	Intra observer agreement, the 95% CI (LCL – UCL)		
	Reader 1	Reader 2	Reader 3
Image quality	0.81 (0.69–0.94)	0.97 (0.91–1.0)	0.88 (0.75–0.97)
Arterial contaminating	1.0 (1.0–1.0)	1.0 (1.0–1.0)	0.98 (0.95–1.0)
Quality of global venous visualization	0.78 (0.72–0.83)	0.86 (0.83–0.88)	0.86 (0.83–0.88)

graded “excellent” by all readers in 65.3% of cases (3 [2, 3] vs. 1 [1, 2], $p < 0.0001$, Table 2).

Contamination with arterial enhancement

For the product 3D PCV, readers 1 and 2 graded the contaminating arterial enhancement as “none” in 100% (24/24) of cases, and reader 3 graded as “moderate” and “severe” in 83.3% (20/24) and 16.7% (4/24) of cases.

For the optimized 3D PCV, readers 1 and 2 graded the contaminating arterial enhancement as “moderate” in 100% cases, reader 3 graded “minimal” in 4.2% (1/24) of cases and “moderate” in 95.8% (23/24) of cases. Overall median arterial contamination in optimized 3D PCV was rated as “moderate” by all readers in 98.6% of cases (2 [1, 2] vs. 2 [1, 3], $p = 0.0004$, Table 2).

Visualization of venous segments

A total of 360 venous segments (180 venous segments for each product and optimized 3D PCV) were evaluated twice by all three readers.

For the product 3D PCV, reader 1 scored 8.1% (29/360) of segments with grade 4, 40.6% (146/360) with grade 3, 17.2% with grade 2 (62/360), and 34.2% (123/360) with grade 1. Reader 2 identified 13.1% (47/360) of segments with grade 4, 34.1% (123/360) with grade 3, 21.4% with grade 2 (77/360), and 31.4% (113/360) with grade 1. Reader 3 rated 13.1% (47/360) of segments with grade 4, 33.9% (122/360) with grade 3, 18.9% with grade 2 (69/360), and 34.2% (123/360) with grade 1. The overall median rating grades [min, max] of all readers were the following: reader 1: 2 [1, 4], reader 2: 2 [1, 4], and reader 3: 2 [1, 4].

For the optimized 3D PCV, reader 1 scored 53.4% (192/360) of segments with grade 4, 29.4% (106/360) with grade 3, 8.6% with grade 2 (31/360), and 8.6% (31/360) with grade 1. Reader 2 identified 36.1% (130/360) of segments with grade 4, 43.9% (158/360) with grade 3, 15.6% with grade 2 (56/360), and 4.4% (16/360) with grade 1. Reader 3 rated 58.1% (209/360) of segments with grade 4, 24.4% (88/360) with grade 3, 17.2% with grade 2 (62/360), and 0.3% (1/360) with grade 1.

scale scoring systems in the section “image analysis.” The confidence interval, lower confidence limit, and upper confidence limit are abbreviated to CI, LCL, and UCL.

The overall median rating grades [min, max] of all readers were the following: reader 1: 4 [1, 4], reader 2: 3 [1, 4], and reader 3: 4 [1, 4].

The visualization quality of venous segments was considered diagnostic (grade ≥ 3) in 47.6 (514/1080) for the product 3D PCV and in 81.8% (883/1080) for the optimized 3D PCV (2 [1, 4] vs. 3 [1, 4], $p < 0.0001$). All venous segments were rated significantly better using the optimized 3D PCV (Table 3).

There was substantial or (near) perfect intra and inter observer agreement for the product and optimized 3D PCV concerning the image quality, contamination with the arterial enhancement, and visualization of venous segments (Tables 2, 3, and 4).

Discussion

In the literature, there are many publications on the visualization of cerebral venous system using MR techniques [14, 16, 20]. In most cases, the use of a contrast-enhanced venography technique was justified due to its better image quality compared to non-contrast-enhanced techniques [16]. However, over the past few years, measurement methods have been investigated, which use a lower dose of contrast agent without significant impairment of image quality [20, 23].

In 2013, Kanda et al. [27] reported about brain signal abnormalities after serial injection of gadolinium-based contrast

Table 3 Inter observer agreement for the evaluation of image quality, arterial contaminating, and visualization of all venous segments of product and optimized 3D PCV based on the introduced 3- and 4-point scale scoring systems in the section “image analysis.” The confidence interval, lower confidence limit, and upper confidence limit are abbreviated to CI, LCL, and UCL

Variable	Inter observer agreement, the 95% CI (LCL, UCL)
Image quality	0.59 (0.58–0.61)
Arterial contaminating	0.85 (0.78–0.91)
Quality of global venous visualization	0.82 (0.80–0.84)

Table 4 Evaluation product versus optimized 3D PCV based on the introduced 3- and 4-point scale scoring systems in the section “image analysis” using Wilcoxon-signed-rank test

Variable	Median [min, max]		<i>p</i> value (product vs. optimized)
	Product	Optimized	
Image quality	1 [1, 2]	3 [1, 3]	< 0.0001
Arterial contaminating	2 [1, 3]	2 [1, 2]	= 0.0004
Global quality of venous visualization	2 [1, 4]	3 [1, 4]	< 0.0001
Segmental quality of venous visualization			
Superior sagittal sinus (1)	4 [1, 4]	4 [3, 4]	= 0.042
Inferior sagittal sinus (2)	2 [1, 4]	3 [1, 4]	< 0.0001
Vein of Galen (3)	3 [3, 4]	4 [3, 4]	< 0.0001
Straight sinus (4)	3 [3, 4]	4 [3, 4]	< 0.0001
Torcular herophili (5)	3 [2, 4]	4 [3, 4]	< 0.0001
Transverse sinus (6)	1 [1, 2]	2 [1, 3]	< 0.0001
Sigmoid sinus (7)	1 [1, 2]	3 [1, 4]	< 0.0001
Superior petrosal sinus (8)	3 [2, 4]	4 [3, 4]	< 0.0001
Cavernous sinus (9)	2 [1, 3]	3 [3, 4]	< 0.0001
Cortical vein (10)	3 [2, 4]	4 [3, 4]	< 0.0001
Internal cerebral vein (11)	2 [1, 3]	4 [3, 4]	< 0.0001
Basal vein of Rosenthal (12)	2 [1, 3]	3 [1, 4]	< 0.0001
Superior ophthalmic vein (13)	1 [1, 1]	2 [1, 4]	< 0.0001
Thalamostriate vein (14)	1 [1, 1]	3 [1, 4]	< 0.0001
Internal jugular vein (15)	3 [1, 4]	4 [2, 4]	< 0.0001

agents for the first time. Although the long-term clinical effect of these gadolinium depositions are yet unknown, the interest for usage of contrast agent-free MR-techniques became even more important and necessary in clinical routine imaging. In addition, a successful use of these techniques requires good image quality, as well as artifact-free visualization of the clinical interesting anatomical structures (e.g., the cerebral venous system).

To our knowledge, there is only one report (abstract) in the literature on the systematic optimization of the 3D PCV imaging for the visualization of cerebral veins: Mimura et al. [28] included 7 healthy volunteers (5 men, 2 women, 21–43 years, mean age, 26.7 years) in their study. Three neuroradiologists graded the visibility of the dural sinuses and the cortical veins. They reported that dural sinuses were best visualized at a V_{enc} value of 15 cm/s and cortical veins at 10 cm/s. The optimal thickness of the saturation slab of 100 mm was determined in their work based on the results of the relative ratio of the arterial to venous signal in a phantom measurement.

In addition, there are two publications about some aspects of the optimization of PCV sequence. Markl et al. [29] presented in a phantom study a generalized model to characterize gradient field nonuniformity and its effect on velocity encoding in phase contrast (PC) MRI. They reported that inhomogeneous gradient fields can introduce deviations from the nominal gradient strength and orientation, and therefore spatially dependent first gradient moments. Resulting errors in the measured phase shifts used for velocity encoding can

therefore cause significant deviations in velocity quantification. The generalized PC velocity reconstruction requires the acquisition of full three-directional velocity information to correct the effect of gradient field distortions.

The optimization of 3D PCV sequence with a radial trajectory as an alternative approach to the conventional cartesian trajectory (i.e., used in this work) was presented by Johnson et al. [30]. The radially undersampled acquisition allows for the acquisition of high-resolution angiograms and velocimetry in dramatically reduced scan times. However, such an acquisition is sensitive to blurring and artifacts from off-resonance and trajectory errors. Based on the presented results by Johnson et al., a dual-echo trajectory can be used to correct these errors based on the information from prescan data coupled with a multi-frequency reconstruction. This statement was evaluated using phantom and in vivo human examinations.

In our study, we optimized a 3D PCV product pulse sequence to improve image quality and reduce artifacts, fulfilling diagnostic criteria for the whole cranio-cervical venous vasculature.

In this single center volunteer study, more healthy volunteers with different ages were included compared to the study of Mimura et al. [28].

From each age decade, two healthy volunteers were examined to optimize the sequence parameters for a wide age range of 21 to 76 years, which represent the wide range of patient age examined in the clinical routine.

In the following, each optimized parameter is discussed briefly:

V_{enc} value In accordance with Mimura et al., our results showed that a V_{enc} value of 15 cm/s is optimal for the visualization of the cranio-cervical veins, in particular for those with much lower blood flow velocities than in the sagittal and transverse sinus veins.

Reduction of arterial contamination In contrast to Mimura et al. [28], we did not observe that a thicker spatial saturation slab (100 mm) provides a better suppression of arterial signal intensity.

A thicker saturation slab (100 instead of 75 mm) increases the total measurement time. Therefore, we decided to use a thinner saturation slab thickness.

Gradient mode The whisper gradient mode is quieter than the normal mode, which is beneficial for brain imaging [31]. As presented by Wilén et al. [19], there are no differences in image quality due to this change of mode. With the activation of RF-spoiler, the background signal intensity was suppressed and the contrast to noise of veins was clearly improved (Fig. 5).

Flip angle The Ernst angle for a gradient echo pulse sequence with a TR of 74.4 and a T_1 value of 1531 ms for blood of male objects at 1.5 T [32] is approximately 18°, which is different to value of 10° that we found experimentally.

Overall, the quality of the 3D PCV images is sensitive to the set range of flow velocities in the pulse sequence. Therefore, this value must be chosen carefully dependent on the expected blood flow velocity range in a specific vessel. Thus, it is advantageous to determine the appropriate range of V_{enc} by performing a 2D ECG-triggered PC flow measurement before a 3D PCV measurement.

Limitation of the study

For the simplification of the recruitment process, only male healthy volunteers were included in this study. No gender-related differences in the visualization of vessels between male and female healthy volunteers are expected.

The total acquisition time for the optimized 3D PCV used in the study is longer than that of the product 3D PCV (10:44 vs. 02:51 min). However, it must be noted that the product protocol has a shorter measurement time due to inappropriate parameter setting for the cranio-cervical imaging. For this volunteer study, a 3D stack with 160 slices to cover all cranio-cervical veins for a big head size (FOV of $332 \times 250 \text{ mm}^2$) was measured. In the clinical routine, the number of slices can be reduced

by up to 30% (112 slices), which translates into reduction in acquisition time about 4 min. However, further efforts can and should be undertaken to reduce scan time while maintaining high image quality but that was beyond the scope of this study.

It should be mentioned that the improved protocol was compared to the product protocol of one manufacturer only. The product protocol, however, was specifically designed by the manufacturer for the application investigated. To avoid the possibility that we optimized a sub-standard product protocol, or that we applied the protocol wrongly, the manufacturer was closely involved in the study.

Conclusions

In conclusion, the optimized protocol presented here allowed contrast agent-free 3D PCV MRI of the cranial veins with unprecedented resolution of the vasculature. In future studies, the optimized 3D PCV should be evaluated in patients with various cerebral venous diseases and in combination with standard invasive/minimal-invasive and non-/contrast-enhanced methods. The purpose of the future studies is to create a non-invasive, contrast-agent-free imaging protocol without or with less ionizing radiation to identify of venous sinus thrombosis.

Acknowledgments The authors thank the MRI technicians in the Department of Radiology and Neuroradiology for their assistance in MR imaging. We quite warmly thank Dr. Klaus Moldenhauer for his patience, his interest in the science and especially for the fact that he made available himself over the course of several weeks as a volunteer for the optimization of this product 3D PCV.

Compliance with Ethical Standards

Funding JBH was funded by the Deutsche Forschungsgemeinschaft (DFG; HO 4604/1-1 and HO 4604/2-1), the Cluster of Excellence EXC306 at Kiel University and the Medical Faculty for the Molecular Imaging North Competence Center (MOIN CC) as core facility for imaging. MOIN CC was funded by a grant of the European Regional Development Fund (ERDF) and the Zukunftsprogramm Wirtschaft of Schleswig-Holstein (Project No. 122-09-053).

Conflict of interest The authors declare that they have no conflict of interest.

Ethical Approval All procedures performed in the studies involving human participants were in accordance with the ethical standards of the institutional and/or national research committee and with the 1964 Helsinki Declaration and its later amendments or comparable ethical standards.

Informed Consent Informed consent was obtained from all individual participants included in the study.

References

- Friedman DI, Liu GT, Digre KB (2013) Revised diagnostic criteria for the pseudotumor cerebri syndrome in adults and children. *Neurology* 81:1159–1165
- Wall M (2017) Update on idiopathic intracranial hypertension. *Neurol Clin* 35:45–57
- Baryshnik DB, Farb RI (2004) Changes in the appearance of venous sinuses after treatment of disordered intracranial pressure. *Neurology* 62:1445–1446
- Rohr A, Bindeballe J, Riedel C, van Baalen A, Bartsch T, Doerner L, Jansen O (2012) The entire dural sinus tree is compressed in patients with idiopathic intracranial hypertension: a longitudinal, volumetric magnetic resonance imaging study. *Neuroradiology* 54:25–33
- Boussier M-G, Ferro JM (2007) Cerebral venous thrombosis: an update. *Lancet Neurol* 6:162–170
- Ferro JM, Canhao P, Stam J, Boussier M-G, Barinagarrementeria F (2004) Prognosis of cerebral vein and dural sinus thrombosis: results of the international study on cerebral vein and dural sinus thrombosis (ISCVT). *Stroke* 35:664–670
- Lee S-K, terBrugge KG (2003) Cerebral venous thrombosis in adults: the role of imaging evaluation and management. *Neuroimaging Clin N Am* 13:139–152
- Kanda T, Nakai Y, Oba H, Toyoda K, Kitajima K, Furui S (2016) Gadolinium deposition in the brain. *Magn Reson Imaging* 34:1346–1350
- Kim M-H, Lee S-Y, Lee S-E, Yang M-S, Jung J-W, Park CM, Lee W, Cho SH, Kang HR (2014) Anaphylaxis to iodinated contrast media: clinical characteristics related with development of anaphylactic shock. *PLoS One* 9:e100154
- Ozturk K, Soylyu E, Parlak M (2018) Dural venous sinus thrombosis: the combination of noncontrast CT, MRI and PC-MR venography to enhance accuracy. *Neuroradiol J* 31:473–481
- Ko SB, Kim D-E, Kim SH, Roh J-K (2006) Visualization of venous systems by time-of-flight magnetic resonance angiography. *J Neuroimaging* 16:353–356
- Leach JL, Strub WM, Gaskill-ShIPLEY MF (2007) Cerebral venous thrombus signal intensity and susceptibility effects on gradient recalled-echo MR imaging. *AJNR Am J Neuroradiol* 28:940–945
- Axel L, Morton D (1987) MR flow imaging by velocity-compensated/uncompensated difference images. *J Comput Assist Tomogr* 11:31–34
- Liauw L, van Buchem MA, Spilt A, de Bruine FT, van den Berg R, Hermans J, Wasser MN (2000) MR angiography of the intracranial venous system. *Radiology* 214:678–682
- Campeau N, Patton A (2013) Enhance 3D phase contrast angiographic magnetic resonance venography of the brain: initial clinical experience in 23 patients. *Proc Int Mag Reson Med* 21
- Pui MH (2004) Cerebral MR venography. *Clin Imaging* 28:85–89
- Dumoulin CL, Hart HR Jr (1986) Magnetic resonance angiography in the head and neck. *Acta Radiol Suppl* 369:17–20
- Hausmann R, Lewin JS, Laub G (1991) Phase-contrast MR angiography with reduced acquisition time: new concepts in sequence design. *J Magn Reson Imaging* 1:415–422
- Wilen J, Hauksson J, Mild KH (2010) Modification of pulse sequences reduces occupational exposure from MRI switched gradient fields: preliminary results. *Bioelectromagnetics* 31:85–87
- Tomasian A, Salamon N, Krishnam MS, Finn JP, Villablanca JP (2009) 3D high-spatial-resolution cerebral MR venography at 3T: a contrast-dose-reduction study. *AJNR Am J Neuroradiol* 30:349–355
- Zuehlsdorff S, Giri S, Edelman RR (2017) Shimming method for magnetic resonance imaging (patent number 20170123027). Siemens Medical Solutions USA, Inc. (Malvern, PA, US), NorthShore University, HealthSystem Research Institute (Evanston, IL, US)
- McGibney G, Smith MR, Nichols ST, Crawley A (1993) Quantitative evaluation of several partial Fourier reconstruction algorithms used in MRI. *Magn Reson Med* 30:51–59
- Nael K, Fenchel M, Salamon N, Duckwiler GR, Laub G, Finn JP, Villablanca JP (2006) Three-dimensional cerebral contrast-enhanced magnetic resonance venography at 3.0 Tesla: initial results using highly accelerated parallel acquisition. *Investig Radiol* 41:763–768
- Krayenbühl H, Yasargil MG (1979) *Zerebrale Angiographie für Klinik und Praxis*: Thieme
- Marasini D, Quatto P, Ripamonti E (2014) Assessing the inter-rater agreement for ordinal data through weighted indexes. *Stat Methods Med Res* 25:2611–2633
- Landis JR, Koch GG (1977) The measurement of observer agreement for categorical data. *Biometrics* 33:159–174
- Kanda T, Ishii K, Kawaguchi H, Kitajima K, Takenaka D (2014) High signal intensity in the dentate nucleus and globus pallidus on unenhanced T1-weighted MR images: relationship with increasing cumulative dose of a gadolinium-based contrast material. *Radiology* 270:834–841
- Mimura S, Iwata N, Yamane T, Hirata Y, Tanino F, Sugihara S et al (2003) Report on the ECR2003 (European congress of radiology): non-contrast intracranial MR venography with 3D-phase contrast imaging: optimization of presaturation pulse and velocity encoding. *Nihon Hoshasen Gijutsu Gakkai Zasshi* 59:823–824
- Markl M, Bammer R, Alley MT, Elkins CJ, Draney MT, Barnett A, Moseley ME, Glover GH, Pelc NJ (2003) Generalized reconstruction of phase contrast MRI: analysis and correction of the effect of gradient field distortions. *Magn Reson Med* 50:791–801
- Johnson KM, Lum DP, Turski PA, Block WF, Mistretta CA, Wieben O (2008) Improved 3D phase contrast MRI with off-resonance corrected dual echo VIPR. *Magn Reson Med* 60:1329–1336
- Baker MA (2013) Reduction of MRI acoustic noise achieved by manipulation of scan parameters – a study using veterinary MR sequences. *Radiography* 19:11–16
- Zhang X, Petersen ET, Ghariq E, de Vis JB, Webb AG, Teeuwisse WM et al (2013) In vivo blood T(1) measurements at 1.5 T, 3 T, and 7 T. *Magn Reson Med* 70:1082–1086